Reactive P/S/N-containing synergistic flame retardant towards eco-friendly durable flame-retardant cotton fabric: Flame-retardant property, durability and mechanism

Peng Wang (wpeng3537@swu.edu.cn)
Southwest University
Jiang Tu
Southwest University
Qianyu Zhao
Southwest University
Jinping Guan
Soochow University
Hang Xiao
Southwest University
Chunhong Wu
Southwest University

Research Article

Keywords: cotton fabric, flame retardancy, synergy, durability, mechanism

Posted Date: July 8th, 2022

DOI: https://doi.org/10.21203/rs.3.rs-1781201/v1

Abstract

Developing eco-friendly durable flame-retardant cotton fabric not only expands its application area, but also caters to the healthy and environmentally friendly concept of consumers. Herein, a reactive P/S/N-containing synergistic flame retardant (PSN) was synthesized to prepare eco-friendly durable flame-retardant cotton fabric through chemical modifying method. ATR-FTIR and NMR data confirmed its successful synthesis of PSN. TGA data showed that PSN triggered the earlier degradation, while facilitated the char formation at high temperature of cotton fabric. Whiteness and tensile data demonstrated that the high-temperature acidic processing environment deteriorated the whiteness and tensile strength of cotton fabric. Flame-retardant data revealed that PSN conferred outstanding flame retardancy, fire safety and durability to cotton fabric. For treated fabric with the add-on of 14.2%, it achieved an LOI value of 36.5% and extinguished spontaneously even after 50 laundering cycles. PHRR, THR and FGI values of treated fabric decreased sharply in comparison with those of the control fabric. TG-FTIR, SEM and XPS analyses confirmed that PSN exhibited high-efficiency flame-retardant behavior because of the synergy between P, S and N elements.

1. Introduction

Textiles have long been used worldwide in consumer applications like costume and furniture decoration (Sawhney et al. 2008). Fire accidents resulted from the combustion of textile are regarded as one of the main causes of financial losses and casualties (Cheng et al. 2021). Cotton fabric has been commonly used as one of the most consumable natural textiles for clothing and textiles because of its inherent properties such as softness, dyeability, comfortableness, biocompatibility and moisture absorption (Ren et al. 2017; Sykam et al. 2021). However, cotton fabric burns violently once ignited, which easily triggers the fire accident. With the upward trend of strict fire safety laws about textiles, the highly flammable nature of cotton fabric seriously restricts its application area. Thus, it is of great practical significance to reduce the fire hazard of cotton fabric through flame-retardant treatment, which will not only broaden its applications, but also guarantee the security of consumer's lives and property.

Researchers all over the world have devoted themselves to the studies of flame retardants since the 1960s (Li et al. 2021). Previously, halogen flame retardants were widely put into use for their high flame retardance (Xu et al. 2019), and most of them scavenged active radicals in the gaseous phase. However, some gases released in the combustion process have been proven to be toxic, corrosive and carcinogenic. Moreover, they can accumulate in organisms and environments, thus threatening the health of human beings and ecological environments. Phosphorus flame retardants are regarded as suitable substitutes to halogen flame retardants. They can be introduced into cotton fabric through impregnation (Bosco et al. 2015), coating (Miao et al. 2021), LBL self-assembly (Magovac et al. 2020; Wang et al. 2020b; Yang et al. 2016), sol-gel (Fu et al. 2021; Lin et al. 2019) and chemical modifying methods. Impregnation method is easy to operate, but the flame retardancy is barely resistant to washing. Coating, LBL self-assembly and sol-gel techniques endow cotton fabric with flame-retardant durability to some extent, while obviously deteriorate the inherent properties like hand feeling, softness and wearing comfort.

Chemical modifying method relies upon the chemical reaction between cellulose and reactive flame retardant, which notably enhances the durability of flame-retardancy based on the formation of covalent bond. Therefore, various researches have been carried out to develop reactive phosphorus flame retardants.

The most commonly reactive phosphorus flame retardant is Pyrovatex CP, which is widely utilized in industries. Pyrovatex CP reacts with cellulose to form covalent bond, conducing to the improvement of durability. Nevertheless, this kind of flame retardant will release carcinogenic formaldehyde during treatment and usage process, which damages the health of human beings (Zhang et al. 2018). Nowadays, the reactive ammonium phosphate ester flame-retardant (APE) has aroused great interest of researchers due to its green synthetic process, eco-friendly nature and P-N synergistic effect. To further improve the efficiency of APE, some excellent researches have been made around the synergy of flame-retardant groups. Zhang et al. reported APEs containing triazine (Wan et al. 2020) and siloxane (Tian et al. 2019) group respectively, which showed high flame-retardant efficiency because of the synergy between flame-retardant groups. Fabrics treated by 30 wt% flame-retardant solutions all achieved higher LOI value around ~ 40%. Recently, our group synthesized a novel APE with phosphine oxide group through a solvent-free one-pot method. The presence of phosphine oxide group sharply improved the efficiency of APE, and fabric with an ultralow add-on of ~ 6% showed a self-extinguished feature (Wu et al. 2022).

The sulfur element has long been incorporated into phosphorous flame retardants to promote the activity of phosphorus (Wang et al. 2020a), and its role varies with oxidation level (Howell and Daniel 2018). For instance, in sulfide or disulfide compounds, the sulfur element contributes to the crosslinking of decomposed polymer by generating sulfur radicals during combustion. The sulfur element in sulfonyl group exerts flame-retardant role by quenching flame-propagating radicals and diluting fuel as it liberates sulfur dioxide in the flame zone. As one of sulfur-containing groups, ammonium sulphonate group has a broad prospect in constructing flame retardants with high efficiency. It decomposes into sulfonic acid and NH_3 when exposed to heat, and exerts gaseous and condensed flame-retardant roles (Coquelle et al. 2014; Mathur et al. 2020). Thus, it is predictable that APE with ammonium sulphonate group may show high flame-retardant efficiency.

N-tris(hydroxymethyl)methyl-2-aminoethanesulfonic acid (TES) has been widely applied in the fields of biochemistry, molecular biology and environmental sciences because of its pH buffering capacity. With hydroxy and sulfonic groups in its structure, it is convenient to construct APE with ammonium sulphonate group by reacting with phosphoric acid and urea. Herein, a novel APE with ammonium sulphonate group (PSN) for eco-friendly durable flame-retardant cotton fabric was synthesized from TES, phosphoric acid and urea under solvent-free condition. It conferred flame-retardant durability to cotton fabric by reacting with cellulose during baking process. The thermal stabilities under N_2 and air atmosphere, physical properties, flame-retardant properties and flame-retardant durability of cotton fabrics were evaluated in detail via TGA, whiteness, tensile, LOI, vertical burning and cone calorimeter tests. What's more, the flame-retardant mechanism was explored comprehensively through analyzing volatile composition during

thermal decomposition and char structure after combustion of treated fabric via TG-FTIR, ATR-FTIR, SEM and XPS tests.

2. Experimental Section

2.1. Materials

Woven cotton fabric (110 g/m^2) was purchased from Chongqing Beibei Market (China). TES was from Shanghai Aladdin Chemical Reagent Co., Ltd. (China). Phosphoric acid (85 wt%), urea, dicyandiamide and anhydrous ethanol were all from Chengdu Kelong Chemicals Co., Ltd. (China).

2.2. Synthesis of PSN

At room temperature, TES (0.24 mol) and phosphoric acid (0.72 mol) were introduced into a 500 ml beaker. The mixture was increased to 150 ^{o}C and stirred for 2 h. After the slow addition of urea (0.96 mol), the mixture was further reacted for 1 h, thus yielding a sticky liquid with white color. The precipitate was observed after pouring the sticky liquid into massive ethanol. After filtration and drying processes, the target product PSN was acquired with a yield of 95%. ATR-FTIR (cm^{-1}): 3199, 1402 (NH_4^+), 2845, 1435 (-CH_2-), 2350 (P-OH), 1257(P = O), 1178 (O = S = O), 1148 (C-N), 1033, 895 (P-O-C), 949 (P-O). ^{1}H-NMR (δ, D_2O, ppm): 3.10–3.20 (H_1), 3.36–3.46 (H_2), 3.59–3.95(H_4, H_5, H_6). ^{13}C-NMR (δ, D_2O, ppm): 37.5 (C_1), 46.5 (C_2), 58.1 (C_3), 61.0 (C_4), 65.2 (C_5), 65.6 (C_6). ^{31}P-NMR (δ, D_2O, ppm): 0.25 (P_a), 1.56 (P_b), 1.86 (P_c). The synthetic route is presented in Scheme 1.

2.3. Preparation of flame-retardant cotton fabric

Scheme 2 shows the preparation route of flame-retardant cotton fabric. Flame-retardant finishing solution was prepared by dissolving PSN, dicyandiamide and urea in deionized water according to the composition listed in **Table 1**. Dicyandiamide acted as the reaction catalyst between PSN and cellulose. Urea served as the fiber expansion agent, which facilitated the penetration of PSN into the fiber. Pristine cotton fabric was immersed into the finishing solution at 50 ^{o}C for 0.5 h, and padded to achieve a wet pickup of 120 wt%. After cured at 175 ^{o}C for 5 min, it was washed with water and dried in an oven at 120 ^{o}C for 30 min.

Table 1
Composition of flame-retardant finishing solution

Sample	PSN (wt%)	Dicyandiamide (wt%)	Urea (wt%)
Control	0	5	0
CT/PSN5	5	5	0.5
CT/PSN10	10	5	1
CT/PSN20	20	5	2

2.4. Characterization

ATR-FTIR spectrum of cotton fabric was obtained by a Thermo Fisher Nicolet iS50 spectrometer. The measured wavenumber ranged from 4000 to 400 cm^{-1}(2 cm^{-1} resolution, 32 scans). The reflector used was a diamond crystal plate.

Sample morphology coated with gold was microphotographed with a Hitachi S-4800 scanning electron microscope at ×300, ×1000, ×2000 magnifications. Simultaneously, the analyses of elemental composition and distribution were obtained on an EDX spectroscopy.

^{1}H, ^{13}C and ^{31}P-NMR spectra of PSN were characterized on a Qone AS400 spectrometer. The test solvent was D_2O, and the obtained ^{1}H-NMR spectrum was calibrated in accordance with the water peak (4.79 ppm).

Thermal stabilities of cotton fabric were carried out on a PerkinElmer TGA 4000 thermal analyzer under N_2 and air atmosphere. Sample was added into an alumina crucible which was placed into a gas atmosphere with a flow rate of 50 mL/min, and heated in the temperature range of 50 to 650 ^{o}C (10 ^{o}C/min ramp rate).

LOI value of cotton fabric was obtained on a M606B oxygen index instrument according to the standard ASTM D2863-2000.

Vertical burning test (VBT) of cotton fabric was performed with a Nantong Sansi YG815B vertical burning tester following the standard ASTM D6413-99. Sample was ignited by the flame with the height of 4 cm, and the application time of flame was set at 12 s.

Cone calorimeter test (CCT) of cotton fabric was carried out on a FTT0007 cone calorimetry following the standard ISO 5660-1. Sample was exposed under the radiant heat flux of 35 kW/m^2.

TG-FTIR analysis of cotton fabric (~ 20 mg) was conducted on a PerkinElmer TGA 4000 thermal analyzer coupled with a Spectrum Two FTIR spectrometer. The volatiles during decomposition were swept into the

IR gas cell through a teflon tube. The temperature of teflon tube was preheated at 250 ^{o}C to avoid gas condensation. Sample was heated over a temperature range from 50 to 650 ^{o}C (10 ^{o}C/min ramp rate). The measured wavenumber region in FTIR test was from 4000 to 500 cm^{-1} (4 cm^{-1} resolution, 4 scans).

XPS analysis of char residue was performed on a Thermo Fischer ESCALAB 250Xi spectrometer with a monochromatic X-ray source of Al Kα.

Tensile test was carried out on a YM065A Tensile Tester in accordance with the standard ASTM D5035-2006. Cotton fabric in warp or weft direction was stretched with a speed of 100 mm/min.

Whiteness of cotton fabric was measured on a Datacolor 650 spectrophotometer following the standard AATCC 110–2000.

Washing resistance test was performed on a soaping fastness tester following the standard AATCC 61-2006 2A. Flame-retardant fabric and 50 stainless balls were added into detergent solution containing 0.15% 1993 WOB detergent. One laundering cycle (LC) of 45 min at 49 ^{o}C equals to five home machine launderings according to the accelerated laundering method.

3. Results And Discussion

3.1. Structure characterization of PSN

Figure 1 presents the ATR-FTIR and NMR spectra of PSN. Absorption peaks of NH_4^+ (3199, 1402), P-OH (2350), C-H (2845, 1435), O = S = O (1178) and P-O-C (1033, 895) are detected in the ATR-FTIR spectrum. In the ^{1}H-NMR spectrum, peaks at 3.10 ~ 3.20, 3.36 ~ 3.46 and 3.59 ~ 3.95 ppm are assigned to protons marked with H_1, H_2 and H_{4-6}, respectively. The corresponding ratio of integrated areas is 1.00: 1.05: 3.10, which is in line with the number ratio of protons. In the ^{31}P-NMR spectrum, three peaks are observed at 0.25, 1.56 and 1.86 ppm, which correspond to P_a, P_b and P_c, respectively. In the ^{13}C-NMR spectrum, six peaks appear at 37.5, 46.5, 58.1, 61.0, 65.2 and 65.6 ppm, which are attributed to C_1, C_2, C_3, C_4, C_5 and C_6, respectively. These data above accord well with the chemical structure of PSN, confirming its successful synthesis.

3.2. SEM-EDX and ATR-FTIR analyses

SEM-EDX technology was used to analyze the morphologies and chemical compositions of cotton fabrics. Figure 2a shows the SEM images at ×300, ×1000 and ×2000 magnifications and element compositions of pure cotton fabric and CT/PSN20. The control fiber shows the flat twisted-ribbon structure in the lengthways. After flame-retardant finishing, the surface morphology of CT/PSN20 is very close to that of the control fabric. This indicates that PSN penetrates the fiber and reacts with cellulose macromolecular chain mostly in the amorphous region of fiber. The EDX data reveal that CT/PSN20 achieves additional N, P and S elements in comparison with the control fabric, which comes from the flame retardant PSN. This also indirectly proves that PSN has been successfully fixed onto cellulose

macromolecular chain. As shown in Fig. 2b, the characteristic absorption peaks of the control fabric are observed at 1028 (C-O-C), 2905 (C-H) and 3334 cm^{-1} (O-H) in the ATR-FTIR spectrum (Gou et al. 2021). By comparison with the spectra of PSN and the control fabric, some additional peaks are visible in the spectrum of CT/PSN20. Absorption peaks of phosphorus bonds appear at 1233 (P = O), 928 (P-O), 831 (P-O-C) and 770 cm^{-1} (P-N). The P-N bond comes from the decomposition of O = P-ONH_4 group at high temperature. The presence of P-O-C bond gives direct evidence that flame retardant PSN has been chemically bonded to cellulose macromolecular chain.

3.3. Thermal and thermo-oxidative degradation behaviors

TGA tests under N_2 and air atmosphere were performed to evaluate the thermal and thermo-oxidative degradation behaviors of the control fabric and CT/PSN20, respectively. The related curves and data are shown in Fig. 3. The 10% mass loss temperature is 314 ^oC for the control fabric, and the char residue at 600 ^oC is 12.4%. The rapid mass loss happens between 300 ~ 400 ^oC, experiencing a mass loss of about 80%. In this stage, the control fabric degrades following two competitive routes. One is the char formation via the dehydration of glycosyl units, and the other is the formation of volatiles like levoglucosan and furan derivatives via the depolymerization of glycosyl units (Alongi et al. 2014). In comparison with the control fabric, CT/PSN20 achieves a lower 10% mass loss temperature, which suggests that PSN moiety triggers the decomposition of cellulose. The PSN moiety in CT/PSN20 degrades earlier than cellulose and produces acids like phosphoric acid and sulfonic acid. These acids trigger the decomposition of cellulose at lower temperatures through the catalytic dehydration effect. As mentioned above, the catalytic dehydration induced by acids contributes to the char formation of cellulose and restrains the production of volatiles, which ultimately enhances the char yield at higher temperatures.

The thermo-oxidative process of the control fabric consists of two steps according to the DTG curve, the corresponding temperatures at maximal mass loss rates are 345 and 472 ^oC, respectively. The first decomposition stage appears at 300 ~ 400 ^oC, and the mass loss was about 73.5%. This stage corresponds to the depolymerization and dehydration of cellulose, yielding volatiles and aliphatic char, respectively. The second stage (400 ~ 650 ^oC) is ascribed to the carbonation and oxidation degradation of preformed aliphatic char, which yield aromatic char and volatile gases (CO_2 and CO), respectively (Alongi et al. 2013; Price et al. 1997). The presence of PSN moiety triggers the decomposition at lower temperatures and enhances the thermo-oxidative stability at higher temperatures of cotton fabric. The 10% mass loss temperature decreases from 304 ^oC for the control fabric to 261 ^oC for CT/PSN20, while the char yield at 600 ^oC increases from 0.7–17.7%. It is reasonable that the acids from the decomposition of PSN moiety catalyze the cellulose dehydration to favor the char formation. The char serves as an oxygen and heat barrier, which restrains the thermo-oxidative degradation of cotton fabric at higher temperatures.

3.4. Physical properties

To assess how the flame-retardant finishing effected the physical properties of cotton fabric, the tensile strength and whiteness of cotton fabrics were measured, as given in Fig. 4. All the data of cotton fabric show remarkable downward trends following the increase of PSN concentration in finishing solution. For instance, the tensile strength in weft direction and whiteness data of the control fabric are 485 N and 94.0, respectively. The corresponding data of CT/PSN10 are 398 N and 86.0, which decrease by 18.0% and 8.5%, respectively. Flame retardant PSN decomposes to generate acids during baking process. The high-temperature acidic processing environment gives rise to the oxidative degradation of cellulose (Li et al. 2019), which deteriorates the whiteness and tensile strength.

3.5. Flame-retardant properties

The add-on value of cotton fabric in Table 2 shows an upward trend following the increase of finishing solution concentration. The LOI value of cotton fabric experiences different degree of enhancement after finishing, and fabric with a higher add-on achieves a higher LOI value. For CT/PSN20, its LOI value reaches up to 36.5%, which is far beyond the flame-retardant standard. Figure 5depicts the combustion images of cotton fabrics during VBT. The control fabric burns quickly once it is ignited, and leaves nothing but a few ashes after test. CT/PSN5 achieves better flame retardancy because of a slower flame spread rate during combustion when compared with the control fabric. For CT/PSN10 and CT/PSN20, they all extinguish automatically without after-flame time. LOI and vertical burning data reveal that PSN greatly improves the flame retardancy of cotton fabric.

Table 2
Add-on, LOI and vertical burning data of cotton fabrics

Sample	Add-on (%)	LOI (%)	Vertical burning data		
			After-flame time (s)	After-glow time (s)	Damaged length (cm)
Control	–	18.3	15	0	30
CT/PSN5	5.1	23.2	3	0	30
CT/PSN10	8.9	28.6	0	0	5.2
CT/PSN20	14.2	36.5	0	0	4.3

As one of common bench-scale fire tests, cone calorimetry test has been widely used to evaluate the combustibility of material in fire scene. Figure 6 depicts the digital images after CCT, the heat release rate (HRR) and total heat release (THR) versus time curves of the control fabric and CT/PSN20. The crucial data draw from CCT are given in Table 3.

Table 3
Cone calorimetry data of the control fabric and CT/PSN20

Sample	Control	CT/PSN20
TTI (s)	5	—
PHRR (kW/m^2)	181.0	46.8
t-PHRR (s)	15	15
THR (MJ/m^2)	2.02	0.89
FGI (kW/(m^2·s))	12.07	3.12
Av-EHC (MJ/kg)	18.69	10.16
Residual mass (%)	1.2	20.5

The control fabric almost burns out and the underlying aluminium foil is visibly observed after CCT, which confirms its high combustibility. In sharp contrast to the control fabric, CT/PSN20 maintains its original shape after CCT, and the char residue thoroughly covers the underneath aluminium foil. The control fabric is ignited at 5 s when exposed to the radiant heat flux. The HRR increases radically to the peak value (181.0 kW/m^2) at 15 s, and the THR over the whole test is 2.02 MJ/m^2. The THR and peak HRR (PHRR) of CT/PSN20 sharply drop to 0.89 MJ/m^2 and 46.8 kW/m^2, experiencing reductions of ~ 56% and ~ 74% in comparison with those of the control fabric, respectively. FGI (the ratio of PHRR to t-PHRR) sharply decreases from 12.07 kW/(m^2·s) for the control fabric to 3.12 kW/(m^2·s) for CT/PSN20. This implies that the presence of PSN postpones the flashover time of cotton fabric, which wins over more escape time for the people trapped in fire accident. Av-EHC refers to the average heat release from the combustion of flammable volatiles produced during the combustion of materials per unit mass (Bai et al. 2011), which can be used to reflect the density of flammable volatiles during combustion. A lower value suggests a lower density of flammable volatiles formed during the combustion of material (Li et al. 2021). As given in Table 3, CT/PSN20 achieves a lower Av-EHC (10.16 MJ/kg vs. 18.69 MJ/kg) but a higher residual mass (20.5% vs. 1.2%) than the control fabric, demonstrating that PSN contributes to reducing the density of flammable volatiles in the flame zone and promoting the char formation. It is possible that PSN moiety in treated fabric releases nonflammable gases like NH_3 and acids like phosphoric acid during combustion, which will be investigated in detail in the following part. The dilution effect of nonflammable gases decreases the density of flammable volatiles in combustion zone, and the catalytic carbonization effect of acids improves the residual mass after combustion. In conclusion, the presence of PSN sharply reduces the fire hazard of cotton fabric.

3.6. Flame-retardant mechanism analysis

3.6.1. TG-FTIR analysis

TG-FTIR analysis provides information about the volatile composition during material decomposition, which is recognized as a useful tool to explore flame-retardant mechanism.

Absorption peaks of water and CO_2 from cellulose dehydration are found at 3567 and 2357 cm^{-1} both in the 3D and 2D TG-FTIR diagrams of the control fabric and CT/PSN20 in Fig. 7a-b. Peaks at 2926, 1750 and 1085 cm^{-1} appear obviously in the FTIR spectra of volatiles for the control fabric, which belong to the typical absorptions of hydrocarbons (C-H), carbonyls (C = O) and ethers (C-O-C) produced from cellulose depolymerization. The maximum absorption peaks of volatiles appear at 24.9 min for CT/PSN20, which is earlier than that for the control fabric. This suggests that PSN triggers the decomposition of cellulose, which is in line with TG data above. Moreover, typical absorption peaks (931 and 967 cm^{-1}) of NH_3 (Battig et al. 2021) emerge in the spectra of volatiles for CT/PSN20, which can be obviously observed in the 2D TG-FTIR diagram. The release of NH_3 contributes to reducing the density of flammable volatiles and oxygen in the combustion region. Figure 7c shows the absorption intensity versus time curves of hydrocarbons, carbonyls and ethers. The maximal absorption intensities of these volatiles for CT/PSN20 are strikingly weaker than those for the control fabric. Impressively, signals of hydrocarbons and ethers nearly disappear. This confirms that the presence of PSN restrains the release of flammable volatiles during the decomposition of cotton fabric. Moreover, absorption peaks assigned to phosphorus- and sulfur-containing groups are not detected in the FTIR spectra of volatiles for CT/PSN20. This implies that phosphorus and sulfur elements mostly exert condensed-phase flame-retardant role.

3.6.2. Surface micromorphology and chemical composition analyses

Figure 8a shows the digital image and surface micromorphology of residual char for CT/PSN20 after VBT. It is difficult to analyze the surface micromorphology of the control fabric after VBT as it burns out. For CT/PSN20, the fabric structure after combustion can be obviously distinguished at 300 times magnification. Interestingly, the fiber surface of char residue clearly appears some protuberances with cavity structure at 2000 times magnification. In fact, cotton cellulose with numerous hydroxy groups is a natural carbon source. The decomposition of PSN releases NH_3, phosphorus- and sulfur-containing acids during combustion, which act as gas source and acid source, respectively. The phosphorus- and sulfur-containing acids promote the cellulose dehydration to form a viscous char layer, and the release of NH_3 expands the char layer to form protuberances with cavity structure on the fiber surface.

The C, O, N, P and S elements are found in the char residue for CT/PSN20 after VBT, as shown in Fig. 8b. The relevant atomic percentages are 70.93%, 18.51%, 7.54%, 2.69% and 0.33%, respectively. To get detail information about the chemical environments of N, P and S elements, the N1s, P2p and S2p XPS spectra were fitted. Three binding energy peaks of P-N (401.2 eV), C-N (400.3 eV) and N-H (398.8 eV) bonds are observed at N1s XPS spectrum (Qu et al. 2020). The nitrogenous components from PSN release NH_3 during combustion, which reacts with P = O bond to form P-N bond. P2p XPS spectrum shows binding energy peaks of P-N (133.4 eV), P-O-C (134.1 eV) and P-O-P (134.8 eV) bonds (Wu et al. 2022). The P-O-P

bond comes from the dehydration of P-OH group. The esterification reaction between O-H and P-OH groups accounts for P-O-C bond formation. Two binding energy peaks at 167.8 and 169.1 eV are observed in the S2p XPS spectrum, which correspond to C-SO_2 and C-SO_3-C groups (Huang et al. 2019; Jiang et al. 2019; Upare et al. 2013), respectively. The C-SO_3-C group stems from reaction between S-OH group in sulfur-containing acid and O-H group in decomposed cellulose. All XPS data demonstrate that PSN releases phosphorus- and sulfur-containing acids during combustion, which promote the char formation by dehydrating and esterifying the decomposed cellulose.

3.6.3. Flame-retardant mechanism

After combined analyses of TG-FTIR data, surface micromorphology and chemical composition of char residue mentioned above, the flame-retardant mechanism is illustrated in Scheme 3. The decomposition of nitrogen-, phosphorus- and sulfur-containing moieties in PSN generate nonflammable gases like NH_3, phosphorus-containing acids (phosphoric acid, polyphosphoric acid, etc.) and sulfonic acid during combustion, respectively. These acids catalyze the formation of viscous P/N-rich char layer by facilitating cellulose dehydration, thus sharply decreasing the amount of flammable volatiles released in the combustion area. The release of nonflammable gases like NH_3 not only deliquates oxygen and flammable volatiles, but also swells the viscous char layer to form a P/N rich intumescent barrier on the fiber surface. This is conducive to decreasing the combustion intensity and isolating unburned matrix from heat and fuel, thus extinguishing the flame.

3.7. Flame-retardant durability

Figure 9a shows the add-on and LOI data of CT/PSN20 after different LCs. As reported above, CT/PSN20 with the add-on of 14.2% obtains an LOI value of 36.5% and self-extinguishes during combustion. The add-on value shows a declining trend with increasing the LC. This means that the flame retardant amount on the fabric decreases because of the hydrolyzation of covalent bond (P-O-C and S-O-C) between cellulose macromolecular chain and PSN during washing process, thus inevitably resulting in the deterioration of flame retardancy. The LOI value sharply drops to 26.4% after 50 LCs, while the flame still self-extinguishes during VBT as shown in Fig. 9b.

Figure 9c shows the SEM images and EDX data of char residue for CT/PSN20 after 50 LCs. Surprisingly, the fiber surface of char residue appears some solid particles rather than protuberances with cavity structure. Moreover, additional sodium element is detected in comparison with the elemental composition of char residue before washing process, and its weight percentage reaches up to 4.4%. It is well known that the 1993 AATCC standard reference detergent WOB mainly consists of alkylbenzene sulfonate as the anionic surfactant and detergent builders including sodium tripolyphosphate, sodium sulfate and sodium silicate. There are lots of sodium ions in the detergent solution, and the residual O = P-OH and -SO_2-OH groups in flame-retardant fabric bind up with sodium ion to form phosphate and sulphonate during washing process. The phosphate and sulphonate lose the ability to transform into acids during

combustion (Luo et al. 2022; Xu et al. 2021; Zhao et al. 2022), thus greatly weakening the catalytic charring effect. In summary, the deterioration of flame retardancy results from covalent bond (P-O-C and S-O-C) hydrolysis and phosphate/sulphonate formation during washing process.

4. Conclusions

In summary, a reactive and high-efficiency flame retardant PSN was synthesized from TES, phosphoric acid and urea. It was employed to prepare eco-friendly durable flame-retardant cotton fabric by reacting with cellulose during finishing. PSN catalyzed the early degradation of cotton fabric, while facilitated the char formation at high temperature. The whiteness and tensile strength of cotton fabric showed remarkable downward trends with the increasing of PSN concentration in finishing solution. PSN exhibited high-efficiency flame-retardant behavior because of phosphorus-sulfur-nitrogen synergy. For treated fabric with the add-on of 14.2%, its LOI value reached to 36.5%, and dropped to 26.4% after 50 LCs. The deterioration of flame retardancy after washing process was ascribed to the covalent bond (P-O-C and S-O-C) hydrolysis and phosphate/sulphonate formation. Treated fabric obtained much lower THR, PHRR and FGI when compared with the control fabric in cone calorimeter test, manifesting its high fire safety. PSN released nonflammable gases and restrained flammable volatiles production, which sharply reduced the density of oxygen and flammable volatiles in the flame zone. It also produced acids in the condensed phase, which dehydrated cellulose to form intumescent and oxygen/heat isolation char layers.

Declarations

Acknowledgments

This work was financially supported by the National Natural Science Foundation of China (Grant No. 21905233), the Science and Technology Innovation Program of Chengdu-Chongqing Economic Circle Construction of Chongqing Education Commission of China (Grant No. KJCX2020008), the Key Laboratory of Flame Retardancy Finishing of Textile Materials, CNTAC (Grant No. Q811580421), the Natural Science Foundation Project of Chongqing (Grant No. cstc2020jcyj-msxmX0437), the Chongqing Higher Education and Teaching Reform Research Project (Grant No. 213063) and the Postgraduate Education and Teaching Reform Research Project of Southwest University (Grant No. SWUYJS216211).

Conflict of interest The authors declare that they have no conflict of interest.

Ethical approval The authors have no statement about ethical approval as this research does not involve humans and animals.

References

1. Alongi J, Carletto RA, Di Blasio A, Carosio F, Bosco F, Malucelli G (2013) DNA: a novel, green, natural flame retardant and suppressant for cotton. J Mater Chem A 1:4779–4785. https://doi.org/10.1039/C3TA00107E
2. Alongi J, Colleoni C, Rosace G, Malucelli G (2014) Sol–gel derived architectures for enhancing cotton flame retardancy: Effect of pure and phosphorus-doped silica phases. Polym Degrad Stabil 99:92–98. https://doi.org/10.1016/j.polymdegradstab.2013.11.020
3. Bai XY, Wang QW, Sui SJ, Zhang CS (2011) The effects of wood-flour on combustion and thermal degradation behaviors of PVC in wood-flour/poly(vinyl chloride) composites. J Anal Appl Pyrol 91:34–39. https://doi.org/10.1016/j.jaap.2011.02.009
4. Battig A, Müller P, Bertin A, Schartel B (2021) Hyperbranched rigid aromatic phosphorus-containing flame retardants for epoxy resins. Macromol Mater Eng 306:2000731. https://doi.org/10.1002/mame.202000731
5. Bosco F, Casale A, Mollea C, Terlizzi ME, Gribaudo G, Alongi J, Malucelli G (2015) DNA coatings on cotton fabrics: Effect of molecular size and pH on flame retardancy. Surf Coat Tech 272:86–95. http://dx.doi.org/10.1016/j.surfcoat.2015.04.019
6. Cheng XW, Zhang C, Jin WJ, Huang YT, Guan JP (2021) Facile preparation of a sustainable and reactive flame retardant for silk fabric using plant extracts. Ind Crop Prod 171:113966. https://doi.org/10.1016/j.indcrop.2021.113966
7. Coquelle M, Duquesne S, Casetta M, Sun J, Zhang S, Bourbigot S (2014) Investigation of the decomposition pathway of polyamide 6/ammonium sulfamate fibers. Polym Degrad Stabil 106:150–157. https://doi.org/10.1016/j.polymdegradstab.2014.02.007
8. Fu C et al (2021) Self-cleaning cotton fabrics with good flame retardancy via one-pot approach. Polym Degrad Stabil 192:109700. https://doi.org/10.1016/j.polymdegradstab.2021.109700
9. Gou TT, Wu X, Zhao QY, Chang S, Wang P (2021) Novel phosphorus/nitrogen-rich oligomer with numerous reactive groups for durable flame-retardant cotton fabric. Cellulose 28:7405–7419. https://doi.org/10.1007/s10570-021-03980-x
10. Howell BA, Daniel YG (2018) The impact of sulfur oxidation level on flame retardancy. J Fire Sci 36:518–534. https://doi.org/10.1177/0734904118806155
11. Huang YJ et al (2019) Mycelial pellet-derived heteroatom-doped carbon nanosheets with a three-dimensional hierarchical porous structure for efficient capacitive deionization. Environ Sci-Nano 6:1430–1442. http://dx.doi.org/10.1039/C9EN00028C
12. Jiang ZP, Shao Y, Zhao P, Wang H (2019) Flexible heteroatom-doped graphitic hollow carbon fibers for ultrasensitive and reusable electric current sensing. Chem Commun 55:12853–12856. http://dx.doi.org/10.1039/C9CC06341B
13. Li N et al (2021) Eco-friendly and intrinsic nanogels for durable flame retardant and antibacterial properties. Chem Eng J 415:129008. https://doi.org/10.1016/j.cej.2021.129008
14. Li SN, Zhong L, Huang S, Wang DF, Zhang FX, Zhang GX (2019) A novel flame retardant with reactive ammonium phosphate groups and polymerizing ability for preparing durable flame retardant and

stiff cotton fabric. Polym Degrad Stabil 164:145–156. https://doi.org/10.1016/j.polymdegradstab.2019.04.009

15. Lin DM, Zeng XR, Li HQ, Lai XJ, Wu TY (2019) One-pot fabrication of superhydrophobic and flame-retardant coatings on cotton fabrics via sol-gel reaction. J Colloid Interf Sci 533:198–206. https://doi.org/10.1016/j.jcis.2018.08.060
16. Luo XL et al (2022) A facile strategy to achieve efficient flame-retardant cotton fabric with durable and restorable fire resistance. Chem Eng J 430:132854. https://doi.org/10.1016/j.cej.2021.132854
17. Magovac E, Jordanov I, Grunlan JC, Bischof S (2020) Environmentally-benign phytic acid-based multilayer coating for flame retardant cotton. Materials 13. https://doi.org/10.3390/ma13235492
18. Mathur P, Sheikh JN, Sen K (2020) Durable flame-retardant wool using sulphamic acid. Polym Degrad Stabil 174:109101. https://doi.org/10.1016/j.polymdegradstab.2020.109101
19. Miao ZW, Yan DP, Zhang T, Yang F, Zhang SK, Liu W, Wu ZP (2021) High-Efficiency Flame Retardants of a P–N-Rich Polyphosphazene Elastomer Nanocoating on Cotton Fabric. ACS Appl Mater Inter 13:32094–32105. https://doi.org/10.1021/acsami.1c05884
20. Price D, Horrocks AR, Akalin M, Faroq AA (1997) Influence of flame retardants on the mechanism of pyrolysis of cotton (cellulose) fabrics in air. J Anal Appl Pyrol 40–41:511–524. https://doi.org/10.1016/S0165-2370(97)00043-0
21. Qu ZC et al (2020) Surface functionalization of few-layer black phosphorene and its flame retardancy in epoxy resin. Chem Eng J 382:122991. https://doi.org/10.1016/j.cej.2019.122991
22. Ren JS, Wang CX, Zhang X, Carey T, Chen KL, Yin YJ, Torrisi F (2017) Environmentally-friendly conductive cotton fabric as flexible strain sensor based on hot press reduced graphene oxide. Carbon 111:622–630. https://doi.org/10.1016/j.carbon.2016.10.045
23. Sawhney APS, Condon B, Singh KV, Pang SS, Li G, Hui D (2008) Modern applications of nanotechnology in textiles. Text Res J 78:731–739. https://doi.org/10.1177/0040517508091066
24. Sykam K, Forsth M, Sas G, Restas A, Das O (2021) Phytic acid: A bio-based flame retardant for cotton and wool fabrics. Ind Crop Prod 164. https://doi.org/10.1016/j.indcrop.2021.113349
25. Tian PX, Lu Y, Wang DF, Zhang GX, Zhang FX (2019) Solvent-free synthesis of silicon–nitrogen–phosphorus flame retardant for cotton fabrics. Cellulose 26:6995–7007. https://doi.org/10.1007/s10570-019-02554-2
26. Upare PP et al (2013) Chemical conversion of biomass-derived hexose sugars to levulinic acid over sulfonic acid-functionalized graphene oxide catalysts. Green Chem 15:2935–2943. https://doi.org/10.1039/C3GC40353J
27. Wan CY, Liu SD, Chen Y, Zhang FX (2020) Facile, one–pot, formaldehyde-free synthesis of reactive NP flame retardant for a biomolecule of cotton. Int J Biol Macromol 163:1659–1668. https://doi.org/10.1016/j.ijbiomac.2020.09.174
28. Wang P, Chen L, Xiao H, Zhan TH (2020a) Nitrogen/sulfur-containing DOPO based oligomer for highly efficient flame-retardant epoxy resin. Polym Degrad Stabil 171:109023. https://doi.org/10.1016/j.polymdegradstab.2019.109023

29. Wang WJ et al (2020b) Constructing eco-friendly flame retardant coating on cotton fabrics by layer-by-layer self-assembly. Cellulose 27:5377–5389. https://doi.org/10.1007/s10570-020-03140-7
30. Wu X, Gou TT, Zhao QY, Chen L, Wang P (2022) High-efficiency durable flame retardant with ammonium phosphate ester and phosphine oxide groups for cotton cellulose biomacromolecule. Int J Biol Macromol 194:945–953. https://doi.org/10.1016/j.ijbiomac.2021.11.149
31. Xu F, Zhang GX, Wang P, Dai FY (2021) A novel epsilon-polylysine-derived durable phosphorus-nitrogen-based flame retardant for cotton fabrics. Cellulose 28:3807–3822. https://doi.org/10.1007/s10570-021-03714-z
32. Xu F, Zhong L, Zhang C, Wang P, Zhang FX, Zhang GX (2019) Novel high-efficiency casein-based P–N-containing flame retardants with multiple reactive groups for cotton fabrics. ACS Sustain Chem Eng 7:13999–14008. https://doi.org/10.1021/acssuschemeng.9b02474
33. Yang JC, Liao W, Deng SB, Cao ZJ, Wang YZ (2016) Flame retardation of cellulose-rich fabrics via a simplified layer-by-layer assembly. Carbohydr Polym 151:434–440. http://dx.doi.org/10.1016/j.carbpol.2016.05.087
34. Zhang FX, Gao WW, Jia YL, Lu Y, Zhang GX (2018) A concise water-solvent synthesis of highly effective, durable, and eco-friendly flame-retardant coating on cotton fabrics. Carbohydr Polym 199:256–265. https://doi.org/10.1016/j.carbpol.2018.05.085
35. Zhao PY, Xu F, Chen YJ, Huang TD, Zhang GX (2022) A novel durable flame retardant for cotton fabrics based on diethylenetriamine. Polym Degrad Stabil 195:109796. https://doi.org/10.1016/j.polymdegradstab.2021.109796

Scheme

Scheme 1 to 3 are available in Supplementary Files section.

Figures

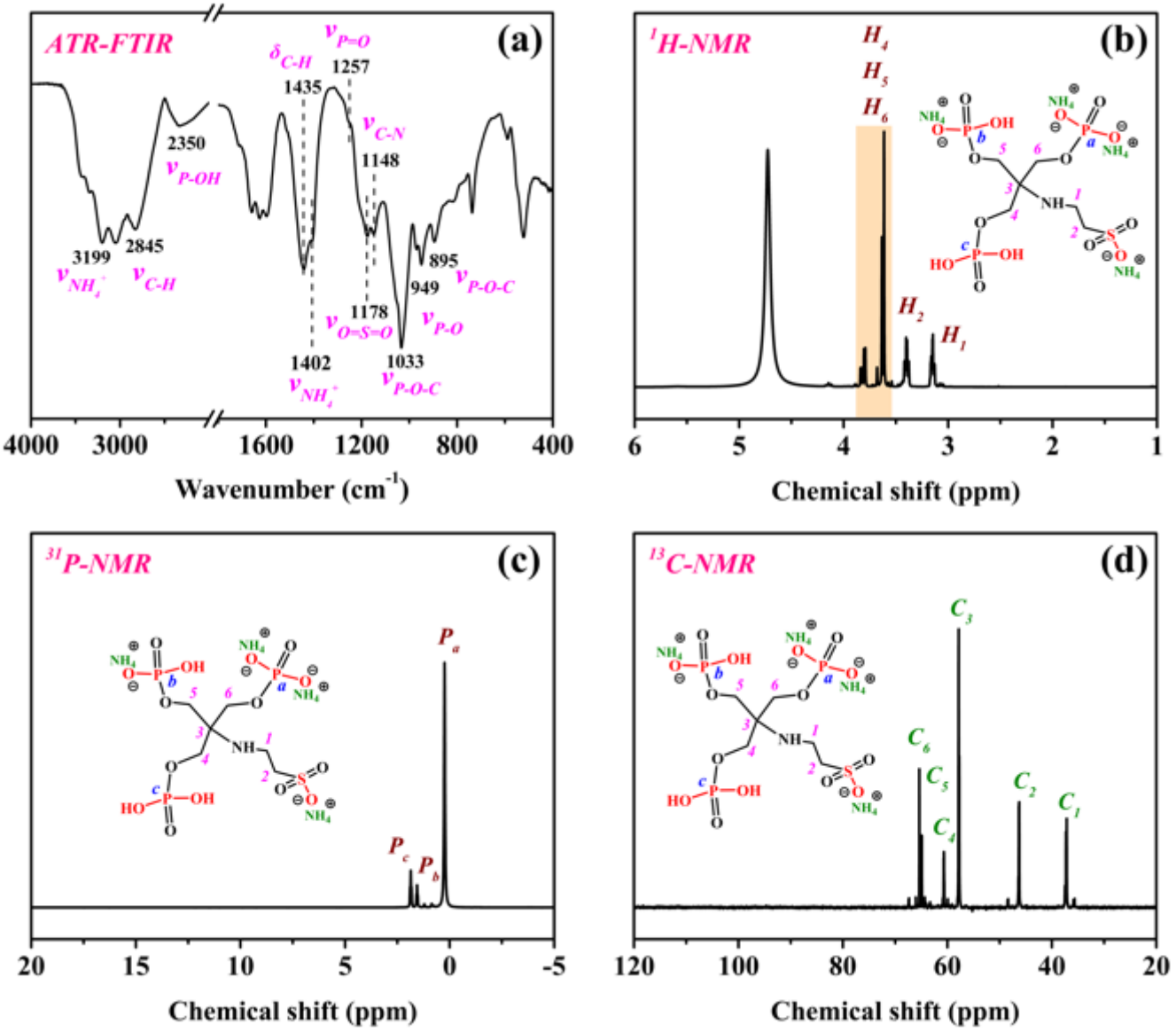

Figure 1

ATR-FTIR (a) and NMR (b-d) spectra of PSN

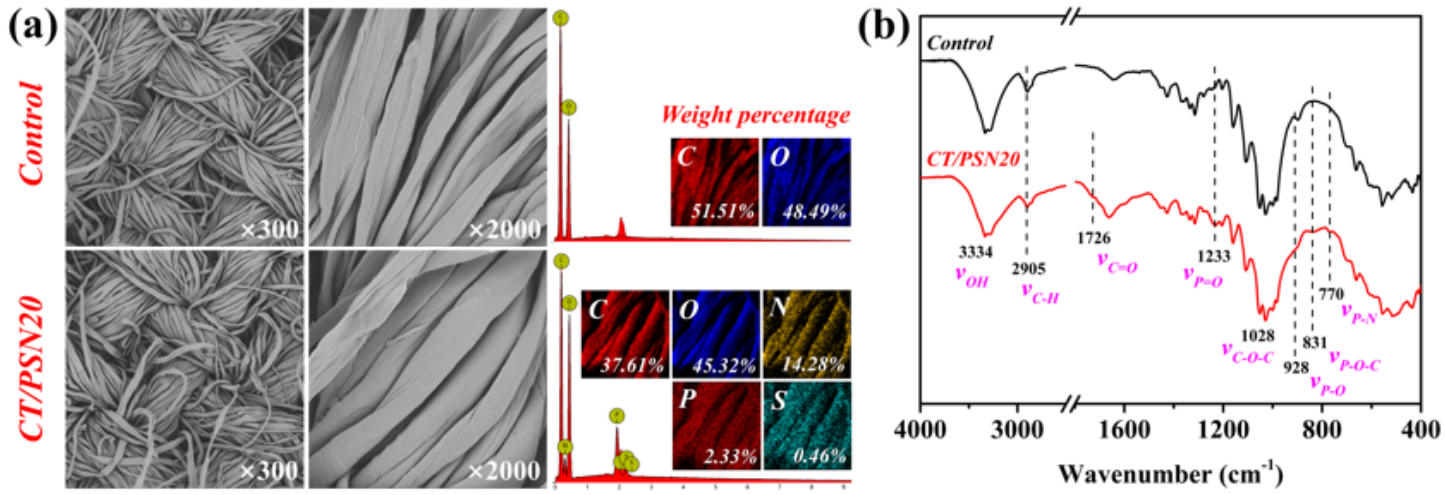

Figure 2

Surface morphologies, element compositions (a) and ATR-FTIR spectra (b) of the control fabric and CT/PSN20

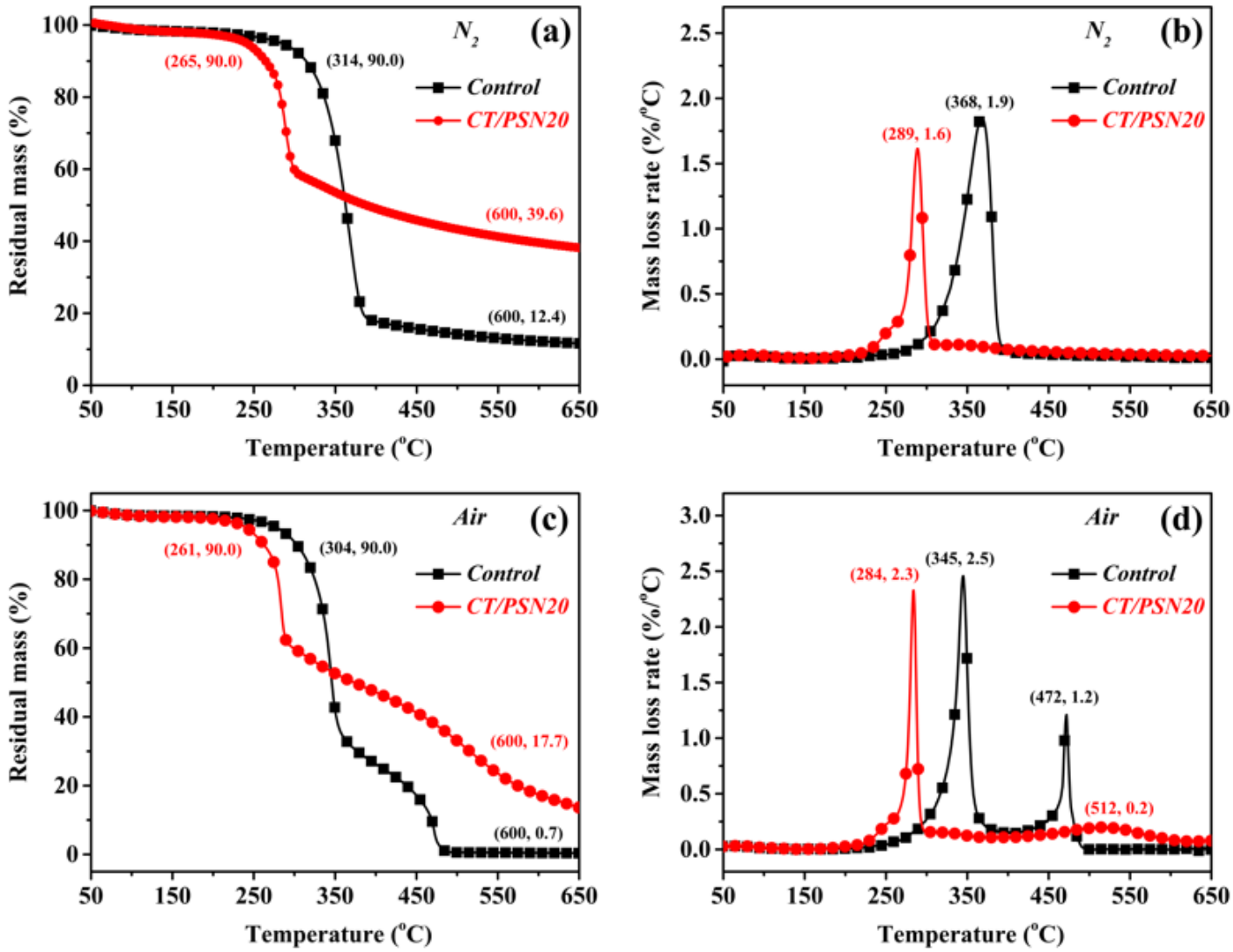

Figure 3

TG and DTG curves of the control fabric and CT/PSN20 under N_2 (a, b) and air (c, d) atmosphere

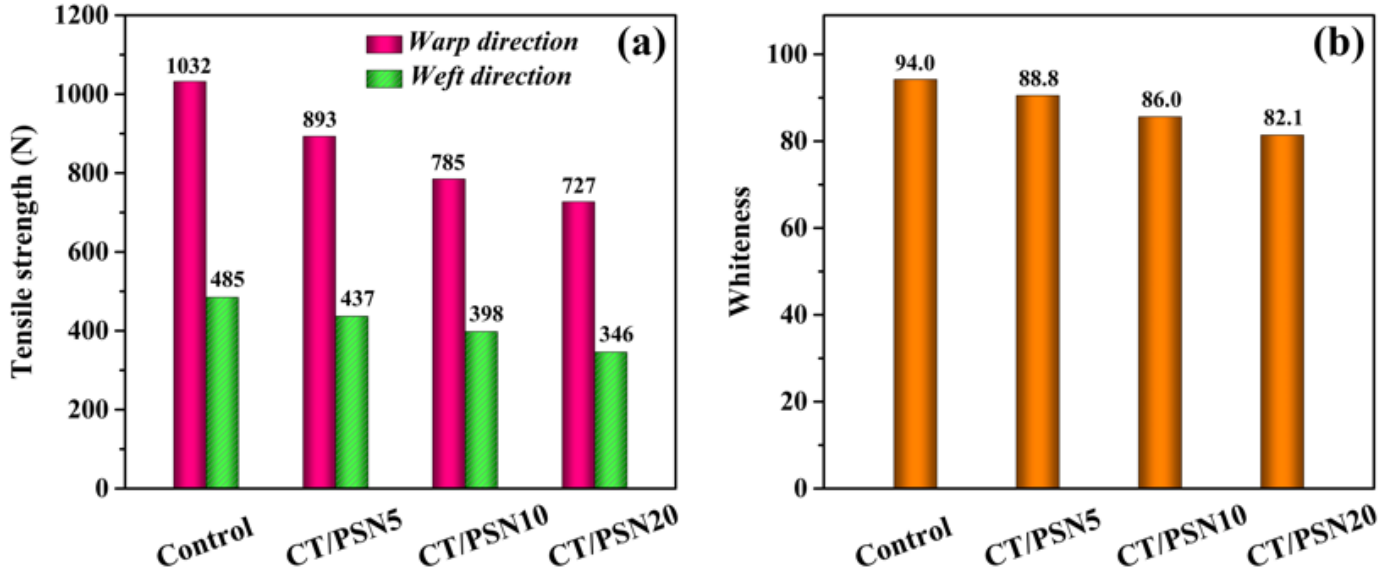

Figure 4

Tensile strength (a) and whiteness (b) data of cotton fabrics

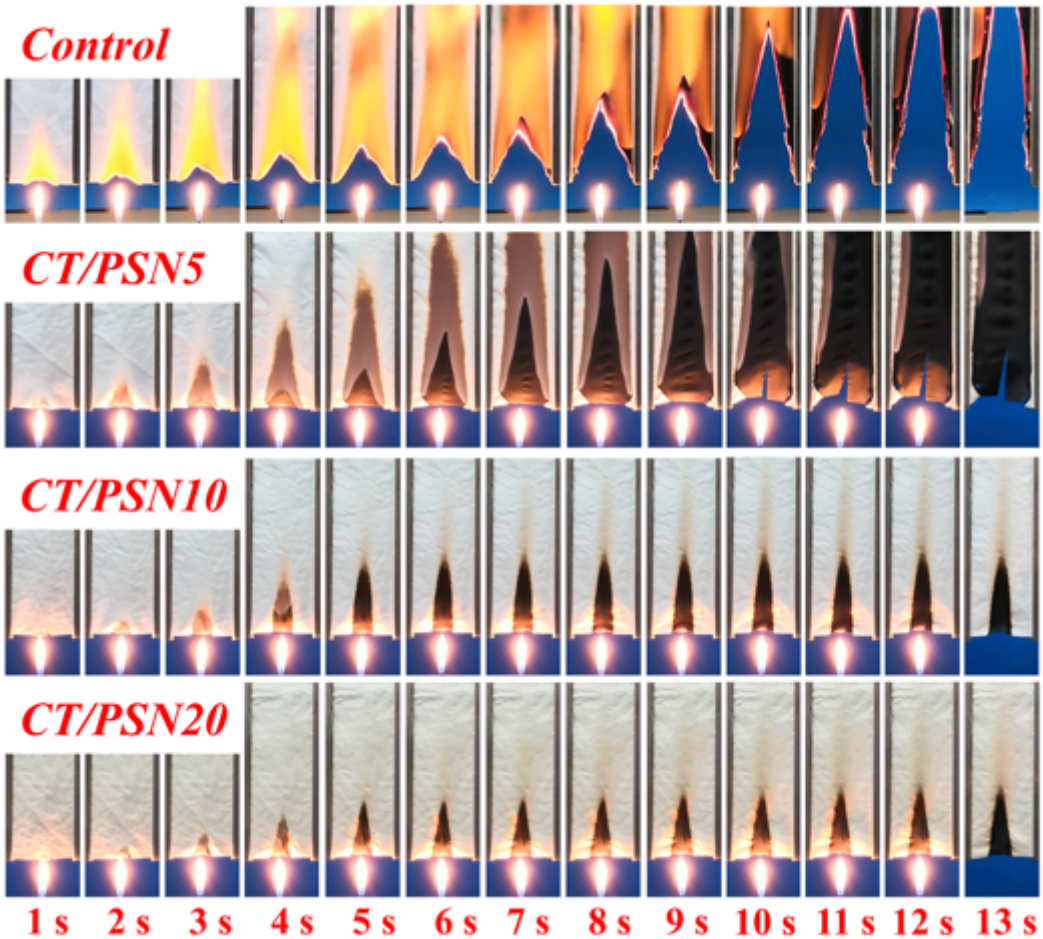

Figure 5

Combustion images of cotton fabrics during VBT

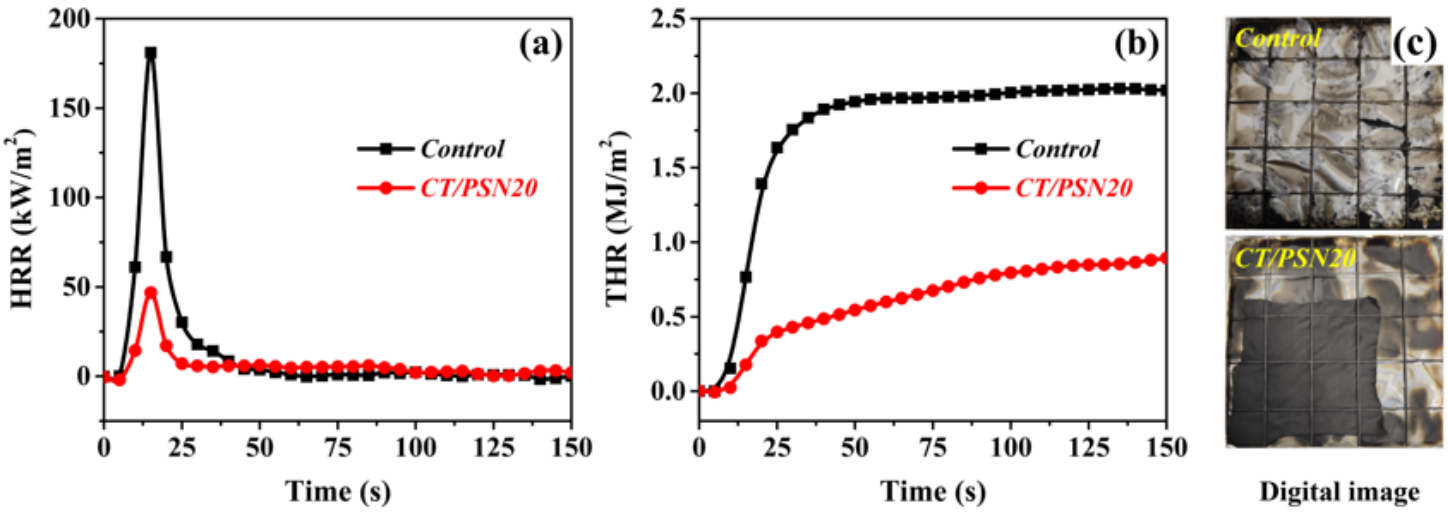

Figure 6

Digital images after CCT, HRR and THR versus time curves of the control fabric and CT/PSN20

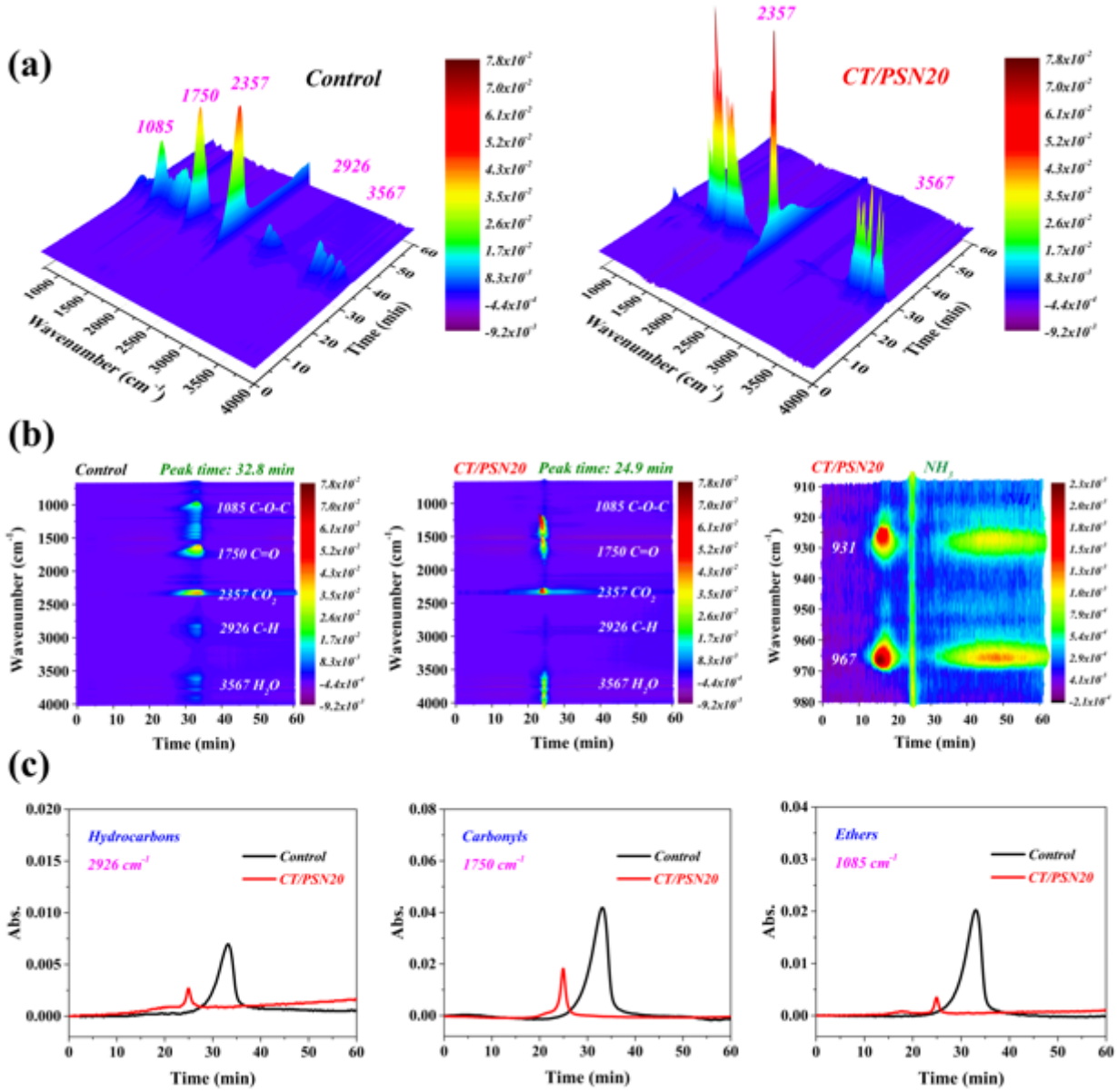

Figure 7

3D (a), 2D (b) TG-FTIR diagrams of the control fabric and CT/PSN20 under N_2 atmosphere; (c) the absorption intensity versus time curves of representative flammable compounds

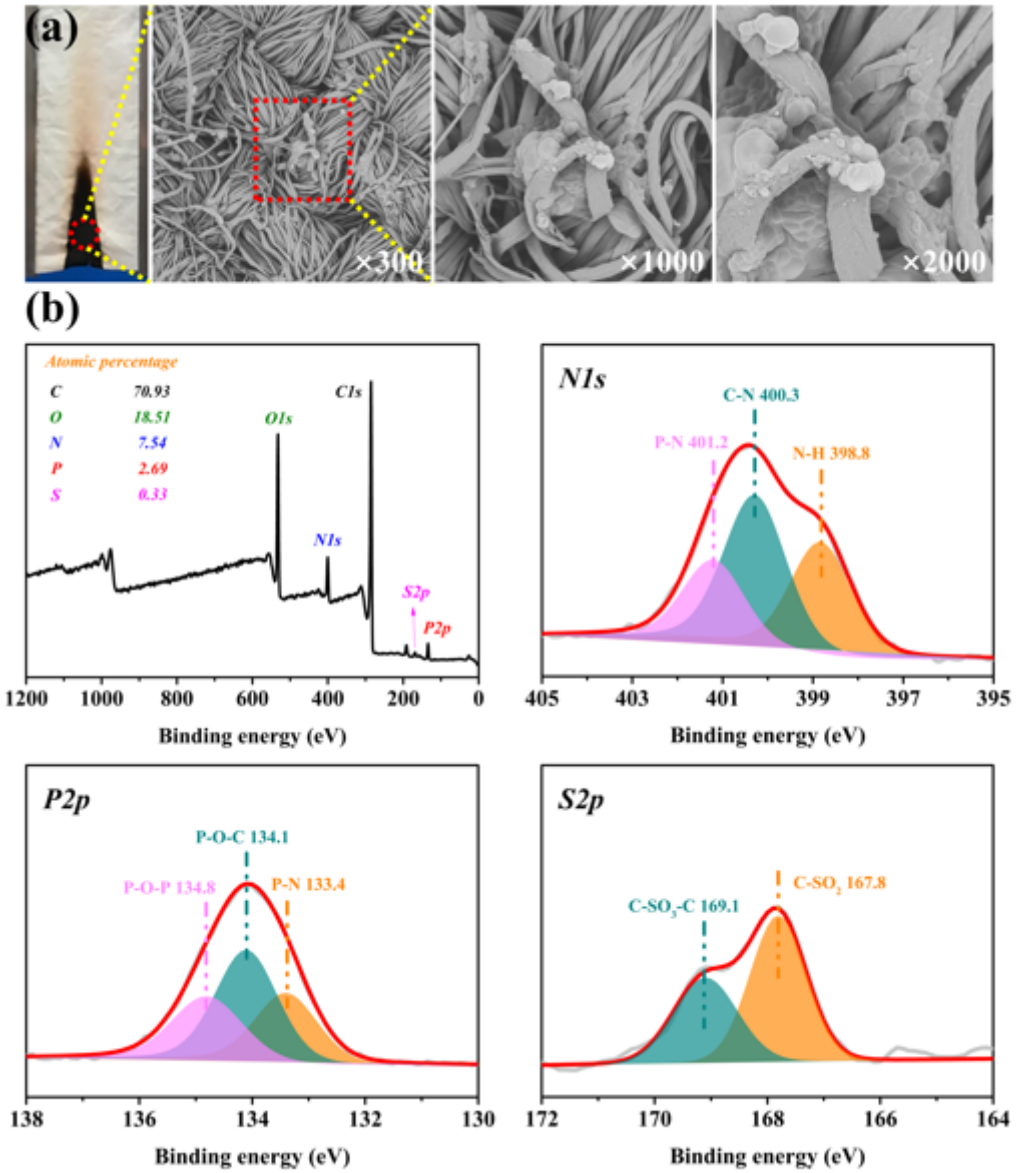

Figure 8

Digital and SEM images (a), XPS spectra and data (b) of char residue for CT/PSN20 after VBT

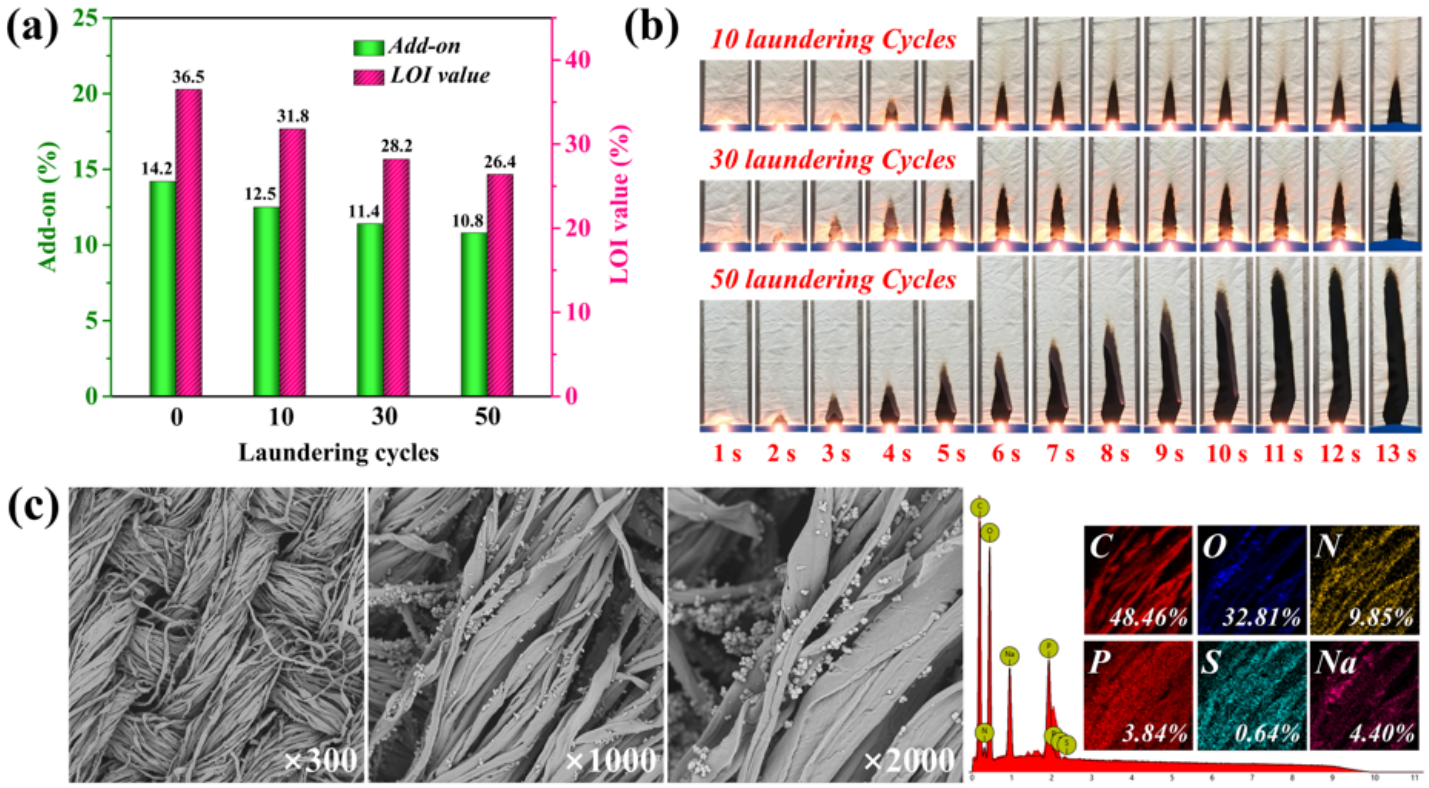

Figure 9

Add-on, LOI data (a) and combustion images (b) of CT/PSN20 after different LCs; (c) SEM images and EDX data of char residue for CT/PSN20 after 50 LCs

Supplementary Files

This is a list of supplementary files associated with this preprint. Click to download.

- Scheme1.png
- Scheme2.png
- scheme3.png